ELSEVIER

Journal of Molecular Catalysis A: Chemical 193 (2003) 285–297

JOURNAL OF MOLECULAR CATALYSIS A: CHEMICAL

www.elsevier.com/locate/molcata

Photocatalytic oxidation of cyanide: kinetic and mechanistic studies

K. Chiang*, R. Amal, T. Tran

Centre for Particle and Catalyst Technologies, School of Chemical Engineering and Industrial Chemistry, The University of New South Wales, Sydney, NSW 2052, Australia

Received 22 July 2002; accepted 20 August 2002

Abstract

The kinetics and mechanism of the photocatalytic oxidation of cyanide in the presence titanium dioxide catalyst were investigated in this study. By displacing the surface hydroxyl groups on the surface of titanium dioxide with fluoride ions, it was deduced that cyanide is oxidised via a pure heterogeneous pathway, i.e. oxidised by the holes trapped at the surface hydroxyl groups $\equiv TiO^{\bullet}$. The quantum efficiency of the photocatalytic oxidation was found to be low (ca. 0.1–0.2%) and this was mainly due to (1) the low adsorption of cyanide ions onto the titanium dioxide surface, (2) the absence of homogenous reaction between cyanide ions and diffused hydroxyl radicals, and (3) the high electron hole recombination rate within the titanium dioxide photocatalyst. A kinetic model was developed to describe the mechanism involved in the photocatalytic oxidation of cyanide.

Keywords: Advanced oxidation technologies; Heterogeneous photocatalysis; Titanium dioxide; Cyanide

1. Introduction

In the past 30 years, extensive research has shown that heterogeneous photocatalysis is a viable alternative to treat wastewater. The degradation of contaminants in wastewater using titanium dioxide photocatalysis is attractive because titanium dioxide could be used repeatedly without any noticeable deterioration of photoactivity and is non-toxic and economical. The kinetics and mechanism of many photocatalytic reactions have been described in detail in the literature and many of these are concerned with the degradation of organic and inorganic compounds present in the wastewater. The photocatalytic oxidation of cyanide ion is one of the most frequently studied reactions due to the acute toxicity of the cyanide ions. One of the earliest studies on heterogeneous photocatalytic oxidation of cyanide was reported by Frank and Bard [1]. In most cases, cyanate is found to be the oxidation product which could be further oxidised simultaneously on the surface of titanium dioxide to produce nitrate and carbonate [2–5]. The hydrolysis of cyanate is also possible which gives rise to ammonium and carbonate as products as shown in Eqs. (1) and (2).

$$CN^- + 2OH^- + 2h_{vb}^+ \overset{TiO_2+UV}{\rightarrow} OCN^- + H_2O \quad (1)$$

$$OCN^- + 2H_2O \rightarrow NH_4^+ + CO_3^{2-} \quad (2)$$

* Corresponding author. Present address: Institute of Environmental Science and Engineering, Nanyang Technological University, Innovation Centre, Block 2, Unit 237, 18 Nanyang Drive, Singapore 637723, Singapore. Tel.: +65-6794-3864; fax: +65-6792-1291.
E-mail address: kchiang@ntu.edu.sg (K. Chiang).

1381-1169/02/$ – see front matter
PII: S1381-1169(02)00512-5

Although many research groups have demonstrated the possibility of degrading cyanide through titanium dioxide photocatalysis, no conclusion can be made in most of these studies on the exact reaction mechanism of cyanide oxidation. The oxidation of cyanide over titanium dioxide has been reported to occur via both direct electron transfer to the holes [2,5–7] and homogeneous hydroxyl radical attack in the bulk solution [8–10]. Therefore, the aim of this work is to investigate the kinetics and mechanism involved to provide further insight into the photocatalytic oxidation of cyanide.

2. Experimental procedures

2.1. Materials and apparatus

The titanium dioxide used in the study was Degussa P25. The primary crystallite size was found to be 30 nm as determined from TEM studies. The material had a surface area of 51 m^2/g and contained predominantly anatase (79% anatase and 21% rutile as determined from X-ray diffraction). Analytical grade sodium cyanide (NaCN) and sodium cyanate (NaOCN) were used as the source of cyanide and cyanate. Nitric acid and sodium hydroxide were used to adjust the pH of solution. Ultra pure gas (either air or N_2) were used in all experiments. All solutions were prepared using freshly prepared Milli-Q water and all chemicals were used without further purification.

The procedure to prepare fluoride-exchanged titanium dioxide is as follow. Sodium fluoride (NaF) was first dissolved into two 500 ml aliquots of water to give a fluoride concentration of 0.02 M. Two suspensions of titanium dioxide were also prepared by adding 5 g of Degussa P25 into two separated 500 ml of water. After sonification for 30 min to break up loosely aggregated particles, one titanium dioxide suspension was mixed with the prepared 500 ml sodium fluoride solution for fluoride exchange reaction. Another blank titanium dioxide slurry was also prepared in the same way except it was mixed with 500 ml of water instead of the sodium fluoride solution. The resultant slurries contained 5 g TiO_2/l and final fluoride concentrations of 0 and 0.01 M, respectively. The pH of the titanium dioxide suspensions was then adjusted to 3.5 by the addition of concentrated nitric acid. According to Minero et al. [11,12] the adsorption of fluoride ions onto titanium dioxide surface occurs most efficiently at a pH of 3.5. The suspensions were mixed well using a rotary shaker at 25 °C for 12 h to allow ion exchange to taken place. The titanium dioxide particles in each suspension was recovered by vacuum filtration and then re-suspended in water to remove any un-adsorbed fluoride ions and nitrate ions on the surface of titanium dioxide. This step was repeated five times in order to remove any un-adsorbed fluoride ions. The ion-exchanged titanium dioxide samples were finally dried in an oven at 110 °C for 12 h and stored under vacuum. The titanium dioxide samples which had been mixed with pure water or exchanged with 0.01 M NaF solution were labelled given the name F0/TiO_2, and F1/TiO_2, respectively, to represent the untreated and fluoride-treated titanium dioxide samples. The fluoride-exchanged titanium dioxide was used in order to study the effect of surface hydroxyl group concentration on the photocatalytic activity of titanium dioxide.

2.2. Photoactivity tests

All experiments were carried out using a 1 l flat bed reactor to assess the photocatalytic degradation of cyanide. Since the pK_a of hydrogen cyanide is equal to 9.3 at 25 °C, it is necessary to work in an alkaline condition in order to avoid the volatilisation of toxic hydrogen cyanide gas during the experiment. Any gaseous hydrogen cyanide formed during the experiment would be captured by a caustic trap (1 M NaOH).

2.2.1. Series 1

The first series of experiment involves the assessment of the photoactivity of titanium dioxide to degrade cyanide. One gram of the titanium dioxide sample was suspended in 500 ml Milli-Q water and sonicated for 30 min. A pre-weighted amount of NaOH was first added to the suspension followed by the addition of NaCN. The volume was then made up to 1 l by further addition of water to reach a pre-determined pH (8.5–12) and cyanide concentrations (0.39–3.85 mM). Unless otherwise stated, air was bubbled through the suspension at a flowrate of 500 ml/min for 15 min before the reaction started. The solution was kept aerated while it was irradiated

for 3–7 h at 30 °C After the complete disappearance of cyanide, the solutions were irradiated further for 2 h more to study the oxidation of cyanate.

2.2.2. Series 2

The pathway of photocatalytic oxidation of cyanide was studied using fluoride-exchanged titanium dioxide. In these experiments, the initial concentration of cyanide was kept at 3.85 mM with the pH varying from 9.5 to 12.0, respectively. The concentration of the photocatalysts (F0/TiO_2 and F1/TiO_2) was kept at 1 g/l. The concentrations of cyanide and cyanate were monitored with time.

2.3. Analysis

The concentration of free cyanide was determined by potentiometric titration using a standardised silver nitrate solution. An automated system consisting of a Metrohm 665 Dosimat and a silver Titrode in conjunction with a 682 Titroprocessor was used to detect the end-point of titration. Samples were first filtered through 0.45 μm syringe filters and 1 ml aliquots were titrated against a standardised $AgNO_3$ solution. This method is suitable to analyse cyanide concentration between 1 and 1000 mg/l CN^- with an accuracy of ±1 mg/l. The concentration of cyanate was determined spectrophotometrically in a buffered 2-aminobenzoic acid solution. The concentration of nitrate was determined by using a Shimadzu high-performance ion chromatography system equipped with a conductivity detector. A Hamilton PRP-X100 inorganic ion column (150 mm × 4.1 mm) was employed for the separation and the mobile phase used was a mixture of 4.0 mM *p*-hydroxybenzoic acid and 2.5% methanol at pH 8.9 and temperature of 30 °C.

A Philips CM200 Field Emission Gun Electron Transmission Microscope FEGTEM were used for micro-structural analysis of the surface of TiO_2. The specific surface areas of all samples were measured using the single point dynamic surface area analyser, which allowed the accurate determination of surface area from 0.5 to 1000 m^2/g. A Cary 5 UV-Vis-NIR spectrophotometer was used to record absorbance data of the solution samples. The Zeta potential of the titanium dioxide samples was measured using the Brookhaven Zetaplus system. Titanium dioxide samples were suspended in 0.01 M NaCl solution at a concentration of 10 ppm. The pH of the solution was adjusted by the addition of NaOH and HCl and the electrophoteric mobility and zeta potential of titanium dioxide particles were determine in the range of pH 3–12.

3. Results and discussion

3.1. Cyanide oxidation by O_2/UV/TiO_2

It has been reported that the initial rate of photocatalytic degradation of many pollutants is a function of the photocatalyst concentration [13–15]. In fact, the reactor configuration plays a key role in determining the photon absorption characteristic of the design and therefore the optimum catalyst concentration. The effect of P25 TiO_2 concentration (0.1–4.0 g/l) on the rate of photocatalytic degradation of cyanide was evaluated at pH 12 and the results are shown in Fig. 1. These results verify that the rate of cyanide degradation increases with TiO_2 loading up to a concentration of 1.0 g/l (or 0.1 wt.%). The enhancement is due to the increasing volumetric photon absorption by the photocatalyst, therefore providing a higher concentration of the charge carrier per unit volume for cyanide oxidation. However, as the loading was increased beyond the optimum value, the degradation rate decreased due to the increased opacity of the suspension and light scattering. The penetration depth of the UV photon is lowered and less titanium dioxide particles could be activated. Therefore, in this study, a TiO_2 loading of 1 g/l corresponding to the highest absorption of incident photons by the photocatalyst was used for subsequent experiments.

It was also found that the rate of photocatalytic degradation of cyanide is dependent on the air flowrate inside the reactor. The aeration process not only provides molecular oxygen to slow down the electron-hole recombination reaction on the titanium dioxide particles, but also facilitates the mixing of photocatalyst in the photoreactor. As shown in Fig. 2, an air flowrate of 500 ml/min provides adequate oxygen concentration and agitation to the system. As shown in Table 1, the adsorption of free cyanide onto titanium dioxide particles (10 g/l) at pH 12 in the absence of light for 24 h is small. This is ascribed to the negative charge of CN^- and a negative surface

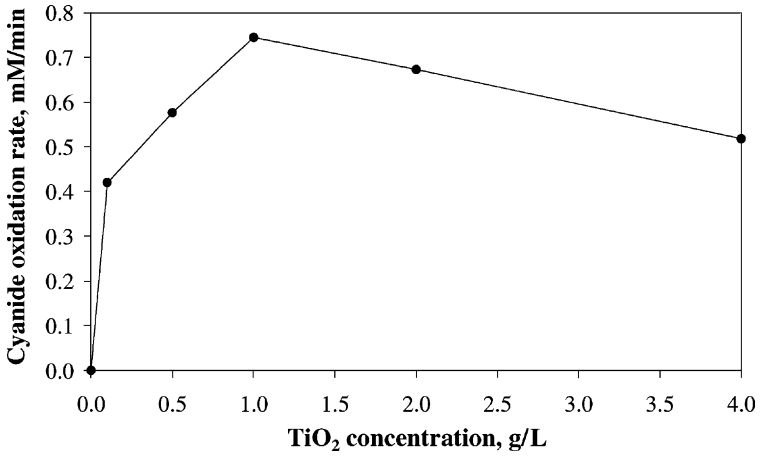

Fig. 1. Effect of titanium dioxide concentration on the rate of photocatalytic cyanide degradation. The solution was at an initial CN^- concentration of 3.85 mM and pH 12.

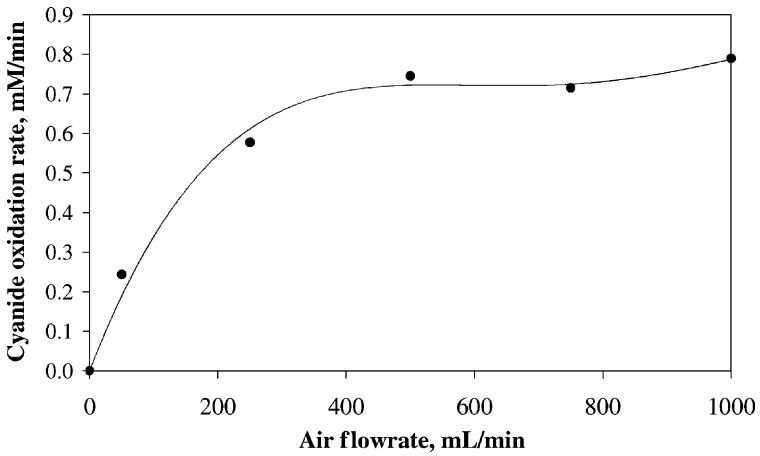

Fig. 2. Effect of air flowrate on the rate of photocatalytic cyanide degradation at 3.85 mM initial CN^- and pH 12.

Table 1
Dark adsorption of cyanide ion for 24 h in the absence and presence (10 g/l) of TiO_2

Initial $[CN^-]$ (mM)	Final $[CN^-]$ (mM)	
	In the absence of TiO_2	In the presence of TiO_2
0.40	0.39	0.35
0.98	0.98	0.87
1.89	1.88	1.73
2.91	2.91	2.79
3.91	3.91	3.71

The initial concentrations of cyanide were 0.40, 1.00, 1.90, 2.89, and 3.90 mM onto and the pH for adsorption was 12.

charge of titanium dioxide particles induced by the adsorption of OH^- ions onto the titanium dioxide surface at high pHs. Fig. 3 shows that the zeta potential of the titanium dioxide particles at pH > 9 in the presence and absence of cyanide ions (3.85 mM) are similar. Any change in the point of zero charge of titanium dioxide at pH lower than 9.3 in the presence of cyanide ions could not be determined due to the possibility of cyanide volatilisation which might affect the accuracy of the measurement. The change in zeta potential therefore confirms that the titanium dioxide surface only interacts and adsorbs cyanide slightly under alkaline condition.

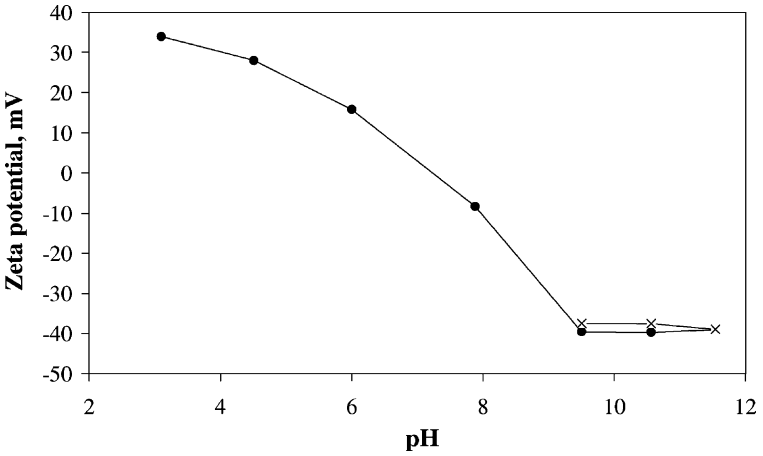

Fig. 3. Zeta potential of P25 TiO_2 in the absence (●) and in the presence (×) of 3.85 mM CN^-. The matrix solution contains 0.01 M NaCl solution.

Similar to other studies, cyanide ion at various concentrations (0.39–3.85 mM CN^-) can be oxidised photocatalytically by titanium dioxide [1,2,5,7–10]. Volatilisation of cyanide in the experiment, as determined from the concentration of cyanide from the caustic trap, was insignificant at the pH and air flowrate used in the experiments. Fig. 4 shows the concentration-time profile of cyanide during the photocatalytic oxidation at pH 12. A constant initial degradation rate of cyanide was observed at a cyanide concentration higher than 2.0 mM and a straight line could best fit the data during the initial course of oxidation. This does not apply for an initial concentration of cyanides below 2.0 mM. Based on the change in cyanide concentration and the number of incident photons impinging on the front window of the reactor cell, the photonic efficiency (ζ_r) of a photocatalytic reaction could be calculated [16,17]. Similarly, the photonic efficiency of cyanide degradation in this study was determined using Eq. (3):

$$\zeta_r = \frac{\Delta[CN^-] \times V \times E_m}{a \times I_0 \times \Delta t} \times 100\% \quad (3)$$

where $\Delta[CN^-]$ is the change in concentration of

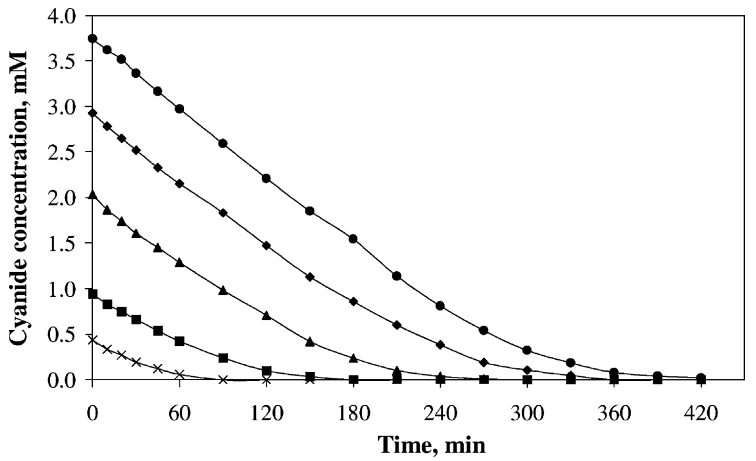

Fig. 4. Concentration profile of cyanide vs. irradiation time at various initial cyanide concentration at 1 g/l TiO_2 and at pH 12. (●) 3.85 mM, (◆) 2.9 mM, (▲) 2 mM, (■) 1 mM, and (×) 0.4 mM.

Table 2
Calculated reaction rate and photonic efficiencies (ζ) obtained from different cyanide concentration at an initial pH of 12

Initial cyanide concentration (mM)	Parameter	
	Rate (M/min)	ζ (%)
0.390	6.18×10^{-6}	0.11
0.944	8.85×10^{-6}	0.15
2.036	1.09×10^{-5}	0.19
2.926	1.18×10^{5}	0.20
3.850	1.25×10^{-5}	0.20

Table 3
Calculated reaction rate constants (k) and photonic efficiencies (ζ) obtained from different pH at an initial cyanide concentration of 3.85 mM

Initial pH of solution	Parameter	
	r (M/min)	ζ (%)
8.5	1.81×10^{-5}	0.29
9.5	1.37×10^{-5}	0.23
10.5	1.32×10^{-5}	0.22
12.0	1.24×10^{-5}	0.21

cyanide expressed in mol/l. A summary of the results for the photocatalytic oxidation of cyanide by P25 TiO_2 is tabulated in Table 2. The values displayed in the table represent the lower limit of the photonic efficiency. It can be seen that these values are generally very low and are always around 0.1–0.2%. The low value of ζ_r is firstly due to the fact that particulate TiO_2 could never absorb all the incident photons. The photons emitted from the UV lamp could be lost through reflection and light scattering due to the high refractive index of titanium dioxide. It is well-known that the reflected photon could sometimes reach 4.5–74% of the incident flux [18] and the theoretical maximum quantity of photon absorption could never exceeds 65% of the incident flux [19]. Secondly, the charge carriers recombination process is fast, especially under high photon flux condition, therefore, consumes the electrons and holes without contributing to any redox reactions. The results in Table 2 show that the photonic efficiency increases when the initial concentration of cyanide in the system increases. It is clear that the photogenerated holes could be scavenged more efficiently in the presence of higher cyanide concentration leading to the increase of the photonic efficiency.

Fig. 5 shows the concentration profiles of cyanide, cyanate, and nitrate during different experiments at different initial cyanide concentrations. It can be seen that as cyanide was being degraded, the concentration of cyanate increased. The concentration of cyanate reached maximum when all the cyanide initially presents in the system was completely degraded. As shown from the carbon mass balance, the sum of cyanide and cyanate ion concentrations at any time during the experiment remained constant. After the completion of cyanide degradation, the solution was further irradiated for 2 h in order to study the degradation of cyanate. The concentration of nitrate was undetectable throughout the experiments and therefore cyanate was confirmed to be the only product of cyanide degradation. Since there was an insignificant change in cyanate concentration at the end of the experiment, it can be concluded that the oxidation of cyanate was insignificant.

The effect of pH on the rate of cyanide oxidation is shown in Table 3 and Fig. 6. As the pH of the solution decreases, the rate of cyanide degradation increases. At pH 8.5, around 66% of the cyanide disappeared through volatilisation as hydrogen cyanide. This was confirmed with the detection of cyanide in the gas trap and the un-closure mass balance of CN^- and OCN^- in the solution at the end of the experiment. Nevertheless, the photocatalytic degradation of cyanide becomes more favourable at lower pH as indicated by the results at pH 9.5, 10.5, and 12. The main cause of the observed lower cyanide degradation rate at high pHs is due to the unfavourable adsorption of cyanide ions onto the more negatively charged surface of titanium dioxide.

3.2. Mechanism of cyanide photooxidation

Many research groups support the direct charge transfer for the photocatalytic oxidation of cyanide by titanium dioxide photocatalyst [1,2,5–7,20]. The oxidation of cyanide via indirect pathway mediates by adsorbed hydroxyl or homogeneous pathway by diffused hydroxyl radical were also reported [8–10]. Reactions (4)–(20) summarise the major elementary reactions which contribute to the overall degradation of cyanide on the surface of titanium dioxide photocatalyst in present study. Both heterogeneous and homogeneous

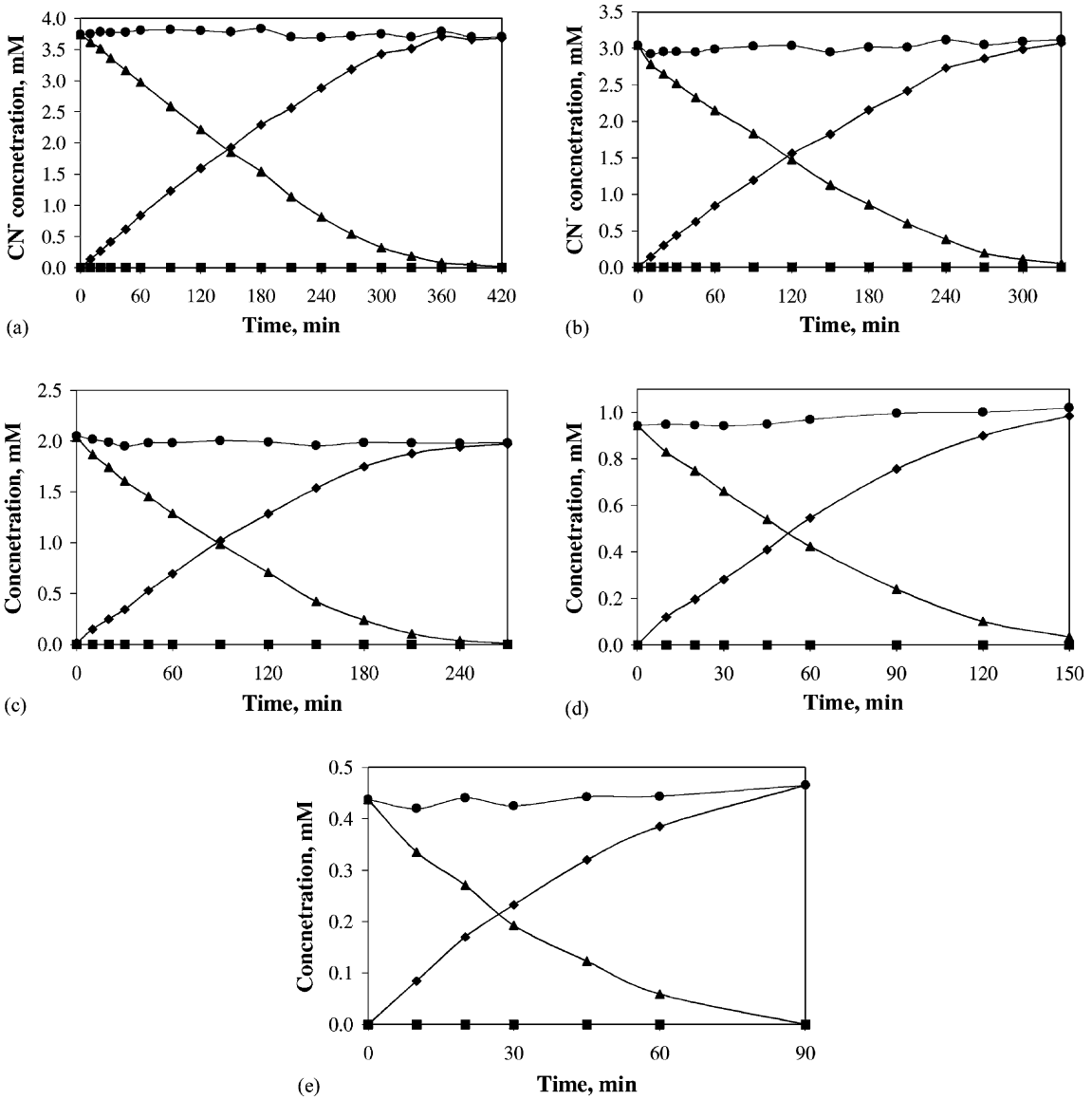

Fig. 5. (a)–(e) Concentration profiles of cyanide and intermediate products plotted against irradiation time at different initial cyanide concentration. (▲) Cyanide concentration, (◆) cyanate concentration, (■) nitrate concentration, and (●) total carbon balance ($CN^- + CNO^-$). The concentration of TiO_2 is 1 g/l and an initial pH of 12. (a) 3.85 mM, (b) 2.89 mM, (c) 1.93 mM, (d) 0.96 mM, and (e) 0.39 mM.

pathways for cyanide oxidation are also considered in the reaction scheme. Reaction (9) and (10) represent the formation of hydroxyl radical $HO^\bullet$ from the reactions between adsorbed hydroxide ion HO^- with h^+_{tr} and $\equiv TiO^\bullet$. The $HO^\bullet$ radicals could diffuse into the bulk solution and react with the cyanide ions to form cyanate ions (OCN^-) and formamide ($HCONH_2$) as shown in reactions (11)–(13). These represent the homogeneous oxidation of cyanide ions in the solution. For direct heterogeneous charge transfer pathway, cyanide ions must be first adsorbed and subsequently react with surface superficial trapped holes h^+_{tr} and

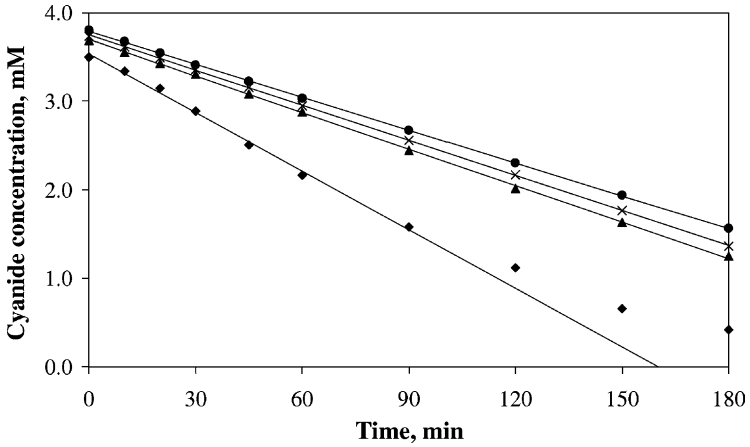

Fig. 6. The influence of pH on the photocatalytic oxidation of cyanide in the presence of 1 g/l TiO_2. (●) At initial pH of 12, (×) at initial pH of 10.5, (▲) at initial pH of 9.5, and (◆) at an initial pH of 8.5.

$\equiv TiO^{\bullet}$ as illustrated in reactions (14)–(17).

$$TiO_2 \xrightarrow{h\nu} TiO_2\{e^-_{cb} \cdots h^+_{vb}\} \quad (4)$$

$$e^-_{cb} + h^+_{vb} \rightarrow \text{heat}/h\nu \quad (5)$$

$$O_2 + H_2O + 2e^-_{cb} \rightarrow HO^- + HO_2{}^- \quad (6)$$

$$h^+_{vb} \xrightarrow{\text{shallow trap}} h^+_{tr^*} \quad (7)$$

$$\equiv TiO^- + h^+_{vb} \xrightarrow{\text{deep trap}} \equiv TiO^{\bullet} \quad (8)$$

$$HO^-_{ads} + h^+_{tr} \rightarrow HO^{\bullet} \quad (9)$$

$$HO^-_{ads} + \equiv TiO^{\bullet} \rightarrow HO^{\bullet} + \equiv TiO^- \quad (10)$$

$$HO^{\bullet} + CN^- \rightarrow HO^{\bullet}CN \quad (11)$$

$$HO^{\bullet}CN \xrightarrow{H_2O} C^{\bullet}ONH_2 \quad (12)$$

$$2C^{\bullet}ONH_2 \rightarrow HCONH_2 + HOCN \quad (13)$$

$$CN^-_{ads} + h^+_{tr} \rightarrow CN_{ads}{}^{\bullet} \quad (14)$$

$$CN^-_{ads} + \equiv TiO^{\bullet} \rightarrow CN_{ads}{}^{\bullet} + \equiv TiO^- \quad (15)$$

$$2CN_{ads}{}^{\bullet} \rightarrow (CN)_2 \quad (16)$$

$$(CN)_2 + 2HO^- \rightarrow OCN^- + CN^- + H_2O \quad (17)$$

$$\equiv TiO^{\bullet} + e^-_{cb} \rightarrow \equiv TiO^- \quad (18)$$

$$2HO_{ads}{}^{\bullet} \rightarrow H_2O_2 \quad (19)$$

$$2H_2O_2 \rightarrow 2H_2O + O_2 \quad (20)$$

It is well known from the radiation chemistry of cyanide that the reaction between $HO^{\bullet}$ radical and cyanide ion leads to the production of formamide radical [21–24]. Upon disproportionation, two formamide radicals yield one cyanate ion and one formamide as final products. If the photocatalytic oxidation of cyanide by titanium dioxide follows a pure homogeneous pathway via $HO^{\bullet}$ radical attack, at least two intermediates will be formed, namely cyanate ions and formamide. In addition their concentrations should be close to, if not equal to, 1:1 stoichiometric ratio. However, as shown from the carbon balance in Fig. 5, the sum of cyanide ion and cyanate ion concentration in the system was always constant and the mass balance was closed. There was no evidence of formation of intermediates other than cyanate ions from the present speciation study. There is no abstractable hydrogen atom in CN^- to react with the $HO^{\bullet}$ radical and there was no evidence of $HO^{\bullet}$ radical addition product formation. These observations suggest that the indirect homogeneous oxidation of cyanide ions by diffuse $HO^{\bullet}$ radicals is not a correct description of the oxidation mechanism. Secondly, if the diffused hydroxyl radical is the active species oxidising cyanide, the oxidation of cyanide ion should become more favourable at a higher pH [25]. This is because as the pH increases, more $HO^{\bullet}$ radicals could be formed and consequently

the oxidation rate of cyanide would be enhanced. However, the opposite trend was observed which strongly support the proposed mechanisms that the photocatalytic oxidation of cyanide is a surface catalysed reaction but not via diffused $HO^{\bullet}$ radicals.

To further consolidate the present postulation, the surface hydroxyl groups on titanium dioxide surface were exchanged with fluoride ions and the sample was used to diagnose the reaction pathway [26–30]. Recently, Minero et al. [11,12] showed that it is possible to differentiate whether the photocatalytic oxidation of phenol proceeds via superficial hydroxyl radical or via a direct interaction with the hole h^{+}_{vb} by the adsorption of fluoride ion on the surface of titanium dioxide. Table 4 and Fig. 7 summarise the results of cyanide oxidation using F0/TiO_2 and F1/TiO_2 at different pHs (9.5, 10.5, and 12.0). It is clear that by incorporating F^{-} ions onto the surface of TiO_2, the photoactivity of titanium dioxide for cyanide degradation decreases and the photonic efficiency is reduced by 25.1, 17.9, and 18.1% at pH 9.5, 10.5, and 12.0, respectively. After fluoride exchange, the concentration of ≡TiOH

Table 4
Calculated reaction rate and photonic efficiencies (ζ) obtained for two type of titanium dioxide samples at 1 g/l and an initial cyanide concentration of 3.85 mM

Parameter	Initial pH of solution		
	9.5	10.5	12.0
(a) F0/TiO_2			
Rate (M/min)	1.21×10^{-5}	1.12×10^{-5}	1.07×10^{-5}
ζ (%)	0.20	0.19	0.19
(b) F1/TiO_2			
Rate (M/min)	9.98×10^{-6}	9.32×10^{-6}	8.48×10^{-6}
ζ (%)	0.17	0.16	0.14

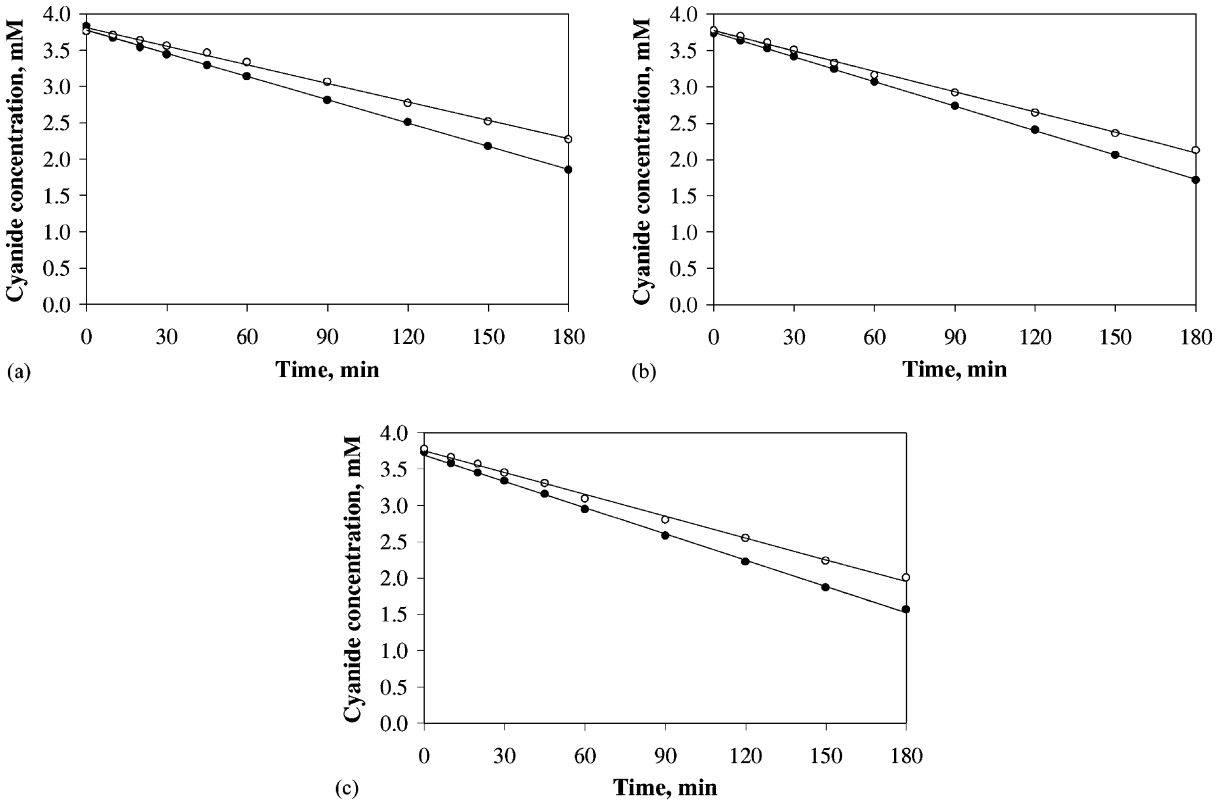

Fig. 7. (a)–(c) The rate of cyanide photooxidation by (●) F0/TiO_2, and (○) F1/TiO_2 at different pH. (a) At pH 12.0, (b) at pH 10.5, and (c) at pH 9.5.

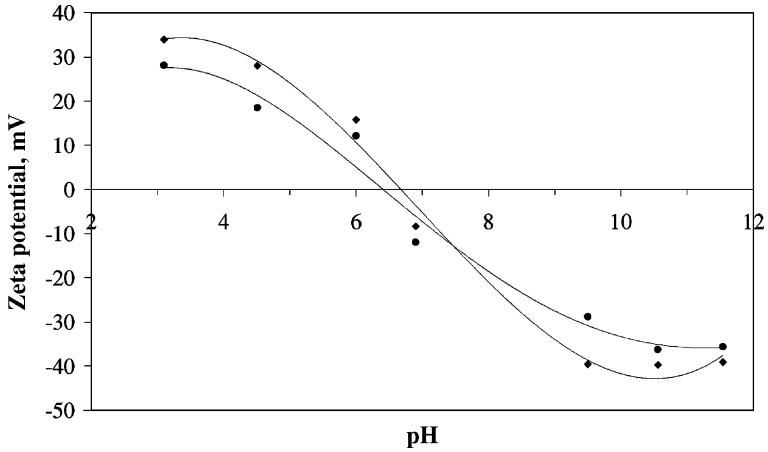

Fig. 8. The pH point zero charge of two different samples. (◆) F0/TiO_2 and (●) F1/TiO_2.

and ≡TiO^- on the titanium dioxide surface decreased due to the irreversible displacement of the basic hydroxyl groups by fluoride ions according to the following reaction.

$$\equiv TiOH + F^- \rightarrow \equiv TiF + HO^- \quad (21)$$

As a result, the ability of the photocatalyst to trap the hole as ≡$TiO^\bullet$ decreases. Although the amount of hydroxyl groups displaced cannot be shown quantitatively, the displacement of surface hydroxyl group on titanium dioxide is evidenced by the shift of pH_{PZC} from 6.68 to 6.41 as shown in Fig. 8. The lowering of the concentration of surface hydroxyl group would induce a higher concentration of untrapped hole or free $HO^\bullet$ radical available for the oxidation of cyanide ion [11,12]. However, no enhancement was observed in this study which means that concentration of surface trapped hole (≡$TiO^\bullet$) is a determining factor for the photocatalytic reaction. As shown previously, no homogenous oxidation of cyanide by hydroxyl radicals was observed and the photocatalytic oxidation of cyanide can only proceed via a pure heterogeneous route, i.e. cyanide can be oxidised by the surface trapped holes. Although the surface trapped hole (≡$TiO^\bullet$) is known to possess a lower oxidation potential than the untrapped holes, it has a longer lifetime which make the oxidation of cyanide ions statistically more favourable compared to the short-life untrapped holes.

3.3. Derivation of reaction kinetics for cyanide oxidation

The essential reactions concluded from the previous discussion are summarised in the following kinetic scheme as illustrated by reactions (R1)–(R13). Since the homogeneous reaction between CN^- ions and free $HO^\bullet$ radicals is unlikely to occur in present system, only the heterogeneous pathway is considered here. The concentration of any species is represented with square brackets "[ ]" in the rate expressions.

$$TiO_2 \xrightarrow{h\nu} TiO_2\{e_{cb}^- \cdots h_{vb}^+\} \xrightarrow{\text{Trapping}} e_{cb}^- + h_{tr}^+ \quad (R1)$$
$$r_1 = k_1\sqrt{I_0} = I^{0.5}$$

$$e_{cb}^- + h_{tr}^+ \rightarrow \text{heat}/h\nu \quad (R2)$$
$$r_2 = k_2[e_{cb}^-][h_{tr}^+] = k_2^*[h_{tr}^+]$$

$$O_2 + H_2O + 2e_{cb}^- \rightarrow HO^- + HO_2^- \quad (R3)$$
$$r_3 = k_3[O_2][e_{cb}^-]$$

$$\equiv TiO^- + h_{vb}^+ \rightarrow \equiv TiO^\bullet \quad (R4)$$
$$r_4 = k_4[\equiv TiO^-][h_{tr}^+] = k_4^*[h_{tr}^+]$$

$$HO_{ads}^- + h_{tr}^+ \rightarrow HO_{ads}^\bullet \quad (R5)$$
$$r_5 = k_5[HO_{ads}^-][h_{tr}^+]$$

$$HO_{ads}^- + \equiv TiO^\bullet \rightarrow HO_{ads}^\bullet + \equiv TiO^- \quad (R6)$$
$$r_6 = k_6[HO_{ads}^-][\equiv TiO^\bullet]$$

$$CN^-_{ads} + h^+_{tr} \rightarrow CN_{ads}{}^\bullet \quad (R7)$$
$$r_7 = k_7[CN^-_{ads}][h^+_{tr}]$$

$$CN^-_{ads} + \equiv TiO^\bullet \rightarrow CN_{ads}{}^\bullet + \equiv TiO^- \quad (R8)$$
$$r_8 = k_8[CN^-_{ads}][\equiv TiO^\bullet]$$

$$\equiv TiO^\bullet + e^-_{cb} \rightarrow \equiv TiO^- \quad (R9)$$
$$r_9 = k_9[\equiv TiO^\bullet][e^-_{cb}] = k^*_9[\equiv TiO^\bullet]$$

$$2CN_{ads}{}^\bullet \rightarrow (CN)_2 \quad (R10)$$
$$r_{10} = k_{10}[CN_{ads}{}^\bullet]^2$$

$$(CN)_2 + 2HO^- \rightarrow CNO^- + CN^- + H_2O \quad (R11)$$
$$r_{11} = k_{11}[(CN)_2][HO^-]^2$$

$$2HO_{ads}{}^\bullet \rightarrow H_2O_2 \quad (R12)$$
$$r_{12} = k_{12}[HO_{ads}{}^\bullet]^2$$

$$2H_2O_2 \rightarrow 2H_2O + O_2 \quad (R13)$$
$$r_{13} = k_{13}[H_2O_2]^2$$

Reaction (R1) represents the photogeneration of electron-hole pair and the rate constant for electron-hole pair generation is k_1 (I_0 is the incident photon flux and I is the rate of photon absorption). Since the UVA lamp (66.7 mW/cm^2 as measured by a UV radiometer) used in the experiments has a photon output higher than the low intensity region (25 mW/cm^2) as defined in the literature, the generation rate is assumed to have a square root dependency of light intensity [31,32]. The photogenerated holes h^+_{vb} will be instantaneously trapped as h^+_{tr} and $\equiv TiO^\bullet$, if not recombined. This process occurs so rapidly in colloidal TiO_2 particles that it does not contribute to the overall kinetics of the charge transfer events and the term trapped hole h^+_{tr} is used in other rate expressions instead of h^+_{vb} to indicate the actual species involved in cyanide photooxidation process.

Reaction (R2) represents the recombination reaction of the photogenerated charges with rate constant k_2. In this study, since the solution was continuously sparged with air, the conduction band electrons e^-_{cb} were efficiently scavenged by molecular oxygen. Therefore, the valence band holes h^+_{tr} would have slightly longer lifetime compared to the e^-_{cb}. Under these circumstances, there would be no significant build-up of electron concentration within the TiO_2 photocatalyst and the rate of recombination reaction (R2) would be dependent on the concentration of h^+_{tr} only [33,34]. Reactions (R3) and (R4) represent the trapping of photogenerated electrons and holes by adsorbed molecular oxygen and surface or adsorbed hydroxyl groups. The rate constant of reaction (R3), k_3, in both air and oxygen saturated titanium dioxide suspension was determined to be 7.6×10^7 l/mol s and the total concentration of hydroxyl groups in Degussa P25 TiO_2 has been shown to be 4.7×10^{-4} mol/g [27,35]. Since these concentrations remain constant on the surface of TiO_2, the term $[\equiv TiO^-]$ can be substituted into k_4 and the rate expression can be simplified by substituting with a second rate constant k^*_4.

During irradiation, the potential electron donors are adsorbed HO^- and CN^- ions and they would interact with the h^+_{tr} and $\equiv TiO^\bullet$ to different extents. As discussed in last section, reactions (R5)–(R13) are the main photocatalytic reactions occurring on the surface of titanium dioxide proposed for this study. In reaction (R5)–(R8), k_5, k_6, k_7, and k_8 are rate constants for the surface oxidation reactions between adsorbed HO^- ions with h^+_{tr}, adsorbed HO^- ions with $\equiv TiO^\bullet$, adsorbed CN^- ions with h^+_{tr}, and adsorbed CN^- ions with $\equiv TiO^\bullet$, respectively. The un-reacted $\equiv TiO^\bullet$ will recombine with e^-_{cb} and return to the ground state as shown in reaction (R9). The rate of this reaction depends on the concentration of $\equiv TiO^\bullet$ on the surface of titanium dioxide and is always a pseudo-first-order with respect to $\equiv TiO^\bullet$ as shown in the rate expression. The reaction of $CN^\bullet$ radicals and the hydrolysis of $(CN)_2$ molecules are shown in reactions (R10) and (R11). The $HO^\bullet$ radicals are also consumed via the formation of H_2O_2 which decomposes rapidly in the presence of TiO_2 and UV irradiation, to give H_2O and O_2 as shown in reaction (R12) and (R13).

Since the $\equiv TiO^-$ groups are the sites for cyanide oxidation, charge transfer will occur at $\equiv TiO^-$. The initial pH of the system and zeta potential measurement indicate that HO^- ions are adsorbed and concentrated near the surface of the titanium dioxide photocatalyst. Since CN^- ions are not well adsorbed on the surface of titanium dioxide, the adsorbed HO^- ions will compete with cyanide ions for the trapped and untrapped holes. This is supported by the findings of Bahnemann et al. [35] who reported that substrate molecules, which are weakly adsorbed on the surface of titanium dioxide, are generally less efficient to react with the holes because the life time of the holes are very short (on

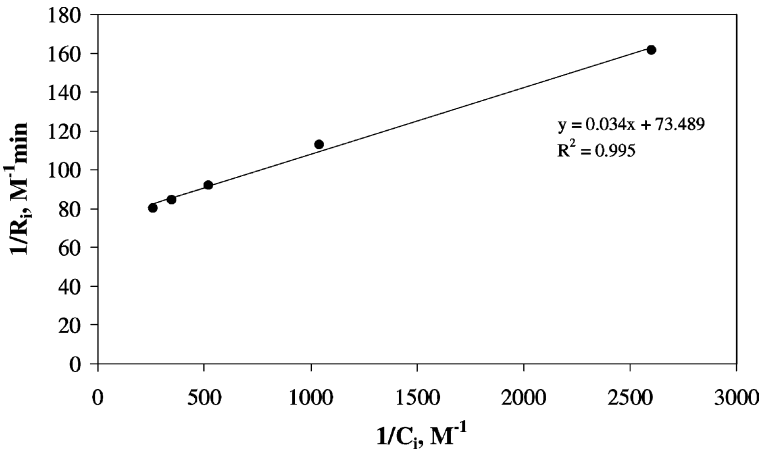

Fig. 9. A plot of the reciprocal of initial cyanide photooxidation rate ($1/R_i$) vs. the reciprocal of initial cyanide concentration ($1/C_i$) at pH 12.

nanosecond range). Due to the low concentration of CN^- ions adsorbed on TiO_2 surface, it is reasonable to assume that the rate of cyanide oxidation by holes is much lower than the oxidation of HO^- by holes. Since O_2 is in surplus, the overall rate of cyanide oxidation would be reaction R8. Summing up, the overall cyanide photooxidation rate (r) can be written as:

$$r = r_8 = k_8[CN^-_{ads}][\equiv TiO^\bullet] \quad (22)$$

By using the relationships of $r_5 \gg r_7$, $[HO^-_{ads}] > [CN^-_{ads}]$, and under steady state concentration of $\equiv TiO^\bullet$, the following rate expression for the photocatalytic oxidation of cyanide ion is obtained:

$$\frac{1}{r} = \left(\frac{k_6[HO^-_{ads}] + k_9^*}{k_8}\right)\left(\frac{k_2^* + k_4^* + k_5[HO^-_{ads}]}{k_4^* I^{0.5}}\right) \times \frac{1}{[CN^-_{ads}]} + \frac{k_2^* + k_4^* + k_5[HO^-_{ads}]}{k_4^* I^{0.5}} \quad (23)$$

It can be seen from Eq. (23) that the rate of cyanide oxidation is dependent on the CN^- ion adsorption on the surface of titanium dioxide. As evidenced by the results from the dark adsorption experiment, cyanide ions are not well adsorbed by titanium dioxide and therefore the mass transfer process plays a significant role in the photocatalytic oxidation of cyanide ions. In accordance to Eq. (23), a plot of the reciprocal of initial cyanide photooxidation rate versus the reciprocal of initial cyanide concentration should be a straight line. Such a plot can be found in Fig. 9 with a correlation coefficient $R^2 = 0.995$ which indicates that there is a good agreement between the prediction of equation and present experimental results. Although Eq. (23) resembles to a conventional reciprocal plot of a Langmuir–Hinshelwood type reaction, it is believed that the parameters in equation are the integrals of the kinetic parameters for all the fundamental reactions (reactions (R1)–(R13)) in present CN^-/TiO_2 system. This behaviour was also reported by Turchi and Ollis [34] on the photocatalytic oxidation of many organic compounds.

4. Conclusion

The kinetics and oxidation mechanism of cyanide in the presence of UV and titanium dioxide catalyst was studied. Cyanide ions were found to be oxidised photocatalytically to cyanate on the surface of titanium dioxide under UV illumination. The photocatalytic oxidation rate of cyanide is dependent on catalyst concentration, air concentration, and initial pH. By displacing the surface hydroxyl groups on the surface of titanium dioxide with fluoride ions, it was confirmed that cyanide is oxidised via a pure heterogeneous pathway at the surface hydroxyl groups. This was explained in terms of the low adsorption of cyanide on titanium dioxide and the longer lifetime of the trapped holes. The photonic efficiency of the

process remains very low and is generally around 0.1–0.2%. Such a low value of photonic efficiency is due to of the lack of interaction of cyanide with the surface of titanium dioxide. In addition, cyanide ions showed low reactivity towards diffused hydroxyl radicals, the majority of the photogenerated holes were not be efficiently scavenged and became recombined. A kinetic expression was developed to model the photocatalytic oxidation reaction.

References

[1] S.N. Frank, A.J. Bard, J. Am. Chem. Soc. 99 (1) (1977) 303.
[2] H. Hidaka, T. Nakamura, A. Ishizaka, M. Tsuchiya, J. Zhao, J. Photochem. Photobiol. A. Chem. 66 (1992) 367.
[3] B.V. Mihaylov, J.L. Hendrix, J.H. Nelson, J. Photochem. Photobiol. A: Chem. 72 (1993) 173–177.
[4] A. Bravo, J. Garcia, X. Domenech, J. Peral, Electrochimica. Acta 39 (6) (1994) 2461.
[5] V. Augugliaro, V. Loddo, G. Marci, L. Palmisano, M.J. Lopez-Munoz, J. Catal. 166 (1997) 272.
[6] T.L. Rose, C. Nanjundiah, J. Phys. Chem. 89 (1985) 3766.
[7] J. Peral, J. Munoz, X. Domenech, J. Photochem. Photobiol. A. Chem. 55 (1990) 251.
[8] N. Serpone, E. Borgarello, M. Barbeni, E. Pelizzetti, P. Pichat, J.M. Hermann, M.A. Fox, J. Photochem. 36 (1987) 373.
[9] M.S. Ahmed, Y.A. Aitta, J. Non-Cryst. Solid 186 (1995) 402.
[10] C.A. Young, in: B. Mishra (Ed.), EPD Congress, The Minerals, Metals and Materials Society, 1998, p. 877.
[11] C. Minero, G. Mariella, V. Maurino, E. Pelizzetti, Langmuir 16 (2000) 2632.
[12] C. Minero, G. Mariella, V. Maurino, D. Vione, E. Pelizzetti, Langmuir 16 (23) (2000) 8964.
[13] A. Mills, S. Morris, R. Davies, J. Photochem. Photobiol. A. Chem. 70 (1993) 183.
[14] H. Kawaguchi, Environ. Technol. 15 (1994) 183.
[15] U. Stafford, K.A. Gray, P.V. Kamat, J. Catal. 167 (1997) 25.
[16] N. Serpone, R. Terzian, D. Lawless, P. Kennepohl, G. Sauve, J. Photochem. Photobiol. A. Chem. 73 (1993) 11.
[17] I. Arslan, I.A. Balcioglu, D.W. Bahnemann, Appl. Catal. B. Environ. 26 (2000) 193.
[18] M. Schiavello, V. Augugliaro, L. Palmisano, J. Catal. 127 (1991) 332.
[19] I. Rosenberg, J.R. Brock, A. Heller, J. Phys. Chem. 96 (1992) 3423.
[20] K. Kogo, H. Yoneyama, H. Tamura, J. Phys. Chem. 84 (1980) 1705.
[21] D. Behar, J. Phys. Chem. 78 (6) (1974) 2660.
[22] B.H.J. Bielski, A.O. Allen, J. Am. Chem. Soc. 99 (18) (1977) 5931.
[23] H. Buchler, R.E. Buhler, R. Copper, J. Phys. Chem. 80 (14) (1976) 1549.
[24] F. Munoz, M.N. Schuchmann, G. Olbrich, V. von Sonntag, J. Chem. Soc., Perkin. Trans. 2 (2000) 655.
[25] C. Galindo, P. Jacques, A. Kalt, J. Photochem. Photobiol. A. Chem. 130 (2000) 35.
[26] H.P. Boehm, Discuss. Fara. Soc. 52 (1971) 264.
[27] J.A. Rob van Veen, F.T.G. Veltmaat, G. Jonkers, J. Chem. Soc., Chem. Commun. (1985) 1656.
[28] K. Kobayakawa, Y. Nakazawa, M. Ikeda, Y. Sato, A. Fujishima, Ber. Bunsenges. Phys. Chem. 94 (1990) 1439.
[29] C. Kormann, D.W. Bahnemann, M.R. Hoffmann, Environ. Sci. Technol. 25 (1991) 494.
[30] A. Hattori, M. Yamamoto, H. Tada, S. Ito, Chem. Lett. (1998) 707.
[31] J.S. Curran, J. Domenech, N. Jaffrezic-Renault, R. Philippe, J. Phys. Chem. 89 (1985) 957.
[32] J.M. Herrmann, Catal. Today 53 (1999) 115.
[33] C. Minero, Catal. Today 54 (1999) 205.
[34] C.S. Turchi, D.F. Ollis, J. Catal. 122 (1990) 178.
[35] D.W. Bahnemann, M. Higendorff, R. Memming, J. Phys. Chem. 101 (1997) 4265.